Orbital Dimer Model for Spin-Glass State in $Y_2Mo_2O_7$

Peter M. M. Thygesen,[1] Joseph A. M. Paddison,[1,2,3,*] Ronghuan Zhang,[1] Kevin A. Beyer,[4] Karena W. Chapman,[4] Helen Y. Playford,[2] Matthew G. Tucker,[2,5,6] David A. Keen,[2] Michael A. Hayward,[1] and Andrew L. Goodwin[1]

[1]*Department of Chemistry, University of Oxford, South Parks Road, Oxford OX1 3QR, U.K.*
[2]*ISIS Facility, Rutherford Appleton Laboratory, Harwell Campus, Didcot, Oxfordshire OX11 0QX, U.K.*
[3]*School of Physics, Georgia Institute of Technology, 837 State Street, Atlanta, Georgia, 30332-0430, U.S.A.*
[4]*Advanced Photon Source, Argonne National Laboratory, Argonne, Illinois 60439*
[5]*Diamond Light Source, Chilton, Oxfordshire, OX11 0DE, U.K.*
[6]*Spallation Neutron Source, Oak Ridge National Laboratory, Oak Ridge, Tennessee 37831, U.S.A.*

(Dated: November 4, 2016)

The formation of a spin glass generally requires that magnetic exchange interactions are both frustrated and disordered. Consequently, the origin of spin-glass behaviour in $Y_2Mo_2O_7$—in which magnetic Mo^{4+} ions occupy a frustrated pyrochlore lattice with minimal compositional disorder—has been a longstanding question. Here, we use neutron and X-ray pair-distribution function (PDF) analysis to develop a disorder model that resolves apparent incompatibilities between previously-reported PDF, EXAFS and NMR studies, and provides a new and physical explanation of the exchange disorder responsible for spin-glass formation. We show that Mo^{4+} ions displace according to a local "2-in/2-out" rule on each Mo_4 tetrahedron, driven by orbital dimerisation of Jahn-Teller active Mo^{4+} ions. Long-range orbital order is prevented by the macroscopic degeneracy of dimer coverings permitted by the pyrochlore lattice. Cooperative O^{2-} displacements yield a distribution of Mo–O–Mo angles, which in turn introduces disorder into magnetic interactions. Our study demonstrates experimentally how frustration of atomic displacements can assume the role of compositional disorder in driving a spin-glass transition.

PACS numbers: 75.50.Lk,61.05.fm,75.10.Nr,75.25.Dk

In a spin-glass transition, spins freeze into a metastable arrangement without long-range order [1–4]. It is generally accepted that two conditions must be satisfied for a spin-glass transition to occur: interactions between spins must be disordered and these interactions must also be frustrated or competing [2, 3, 5, 6]. In canonical spin glasses—*e.g.*, dilute magnetic alloys such as $Cu_{1-x}Mn_x$ [7] and site-disordered crystals such as Fe_2TiO_5 [8]—the nature of the structural disorder that causes disorder in magnetic interactions is well understood. However, spin-glass behaviour is also observed in apparently well-ordered crystals where the geometry of the magnetic lattice alone can generate frustration [9–11]. Here, the mechanism of spin-glass formation poses an important challenge for theory [12–14]. The prototypical material that shows this anomalous behaviour is $Y_2Mo_2O_7$—a system with apparently unremarkable levels of structural disorder, but with thermodynamic properties indistinguishable from canonical spin glasses [15].

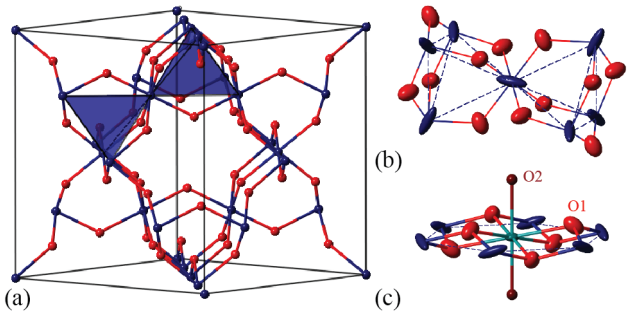

FIG. 1: (a) Crystal structure of $Y_2Mo_2O_7$ generated from the model of [29]: Mo in dark blue, O1 in red, and Y and O2 omitted for clarity. (b) Coordination environment of Mo^{4+} shown with displacement ellipsoids at 50% probability. Prolate Mo^{4+} displacement ellipsoids point along the local-$\langle 111\rangle$ axes (towards the centres of adjacent tetrahedra). (c) Coordination environment of Y^{3+} (green).

The structure and dynamics of $Y_2Mo_2O_7$ have been extensively studied. The conventional nature of the spin-glass transition (freezing temperature $T_f = 22\,K$ [16]) has been shown by measurements including non-linear susceptibility [16, 17], specific heat [18, 19], a.c. susceptibility [20], thermo-remanent magnetization [21–23], inelastic neutron scattering [24], muon-spin rotation (μSR) [25], and neutron spin echo [26, 27]. Neutron-diffraction measurements show that the average structure is well-described by the ordered pyrochlore model (space group $Fd\bar{3}m$) both below and above T_f [28, 29]. In this structure, the average positions of magnetic Mo^{4+} ions describe a network of corner-sharing tetrahedra [Fig. 1(a)]. There are two inequivalent O sites, O1 and O2; each Mo^{4+} is octahedrally coordinated by O1 [Fig. 1(b)], and each Y^{3+} is coordinated by six O1 and two O2 [Fig. 1(c)]. Each pair of Mo neighbours is bridged by a single O1, forming the main magnetic superexchange pathway. The degree of site-mixing and O non-stoichiometry is too small to measure [28, 29] and is calculated to be minimal ($\sim$1%) [30].

A plausible explanation for spin-glass formation invokes local Mo^{4+} displacements to generate variation in exchange interactions [31]. Arguably the clearest experimental signature of anomalies on the Mo site is its large and anisotropic atomic displacement parameter (ADP) obtained from Rietveld

refinement to powder neutron-diffraction data [29] [Fig. 1(b)]. Consistent with this, an EXAFS study (Mo and Y K-edges) showed a large static variance in Mo–Mo distances, $\sigma^2_{\rm stat} = 0.026(5)\,\text{Å}^2$ [32]. Two ^{89}Y NMR studies revealed a distribution of Y environments that was interpreted in terms of a local distortion of the Mo site [31, 33], an explanation supported by μSR experiments [34]. There is a problem with this proposal, however: a state-of-the-art study using neutron pair-distribution function (PDF) analysis found no evidence for local Mo displacements [29]. Instead, it showed variation in Y–O1 distances consistent with a local splitting of the O1 site—a result interpreted as contradicting the EXAFS study [29, 32].

In this Letter, we argue that a disorder model that reconciles these apparently-contradictory results can explain the exchange disorder responsible for spin-glass formation in $Y_2Mo_2O_7$. We critically reassess the key assumption [29] that the absence of obvious Mo–Mo splitting in the PDF implies that local Mo displacements do not occur. We show that the PDF is actually better represented by a model in which Mo ions are displaced, consistent with EXAFS [32], and these Mo displacements are coupled to O1 displacements. In our model, Mo displacements obey a "2-in/2-out" rule on each Mo_4 tetrahedron. This can be interpreted as the formation of Mo–Mo dimers, driven by orbital interactions between Jahn-Teller active Mo^{4+} ions. These orbital dimers do not show long-range order because the pyrochlore lattice supports a macroscopic degeneracy of dimer coverings; this same type of degeneracy is responsible for, *e.g.*, magnetic disorder in spin-ice materials [44]. Because Mo–Mo dimer coverings are disordered and coupled with O1 displacements, there is a disordered arrangement of Mo–O1–Mo bond angles, which introduces sufficient variation in magnetic exchange interactions [12, 13] to explain spin-glass formation.

Our paper is structured as follows. After describing our experiments, we first reproduce the best fit to PDF data obtained previously [29]. We then describe the simplest orbital-dimer model, which is a crystalline approximant to a more complex disordered state. We demonstrate that this model yields a better fit to PDF data than the previous model [29], for the same number of structural parameters. Finally, we show that our model is consistent with previous experimental studies [31–33] and with theoretical requirements for spin-glass formation.

A polycrystalline sample of $Y_2Mo_2O_7$ (8 g) was prepared by firing stoichiometric amounts of Y_2O_3 and MoO_2 for 12 hours at 1400 °C using CO/CO_2 as buffer gas [35]. The value of T_f determined from measurements of the field-cooled and zero-field-cooled magnetization was consistent with the previously-reported value (22 K) [36]. Neutron and X-ray total-scattering data were collected on the POLARIS instrument at ISIS [37] and the 11-ID-B beamline at the APS, respectively. All data were corrected for background scattering and absorption using the GUDRUN program [38] (based on the ATLAS routines [39]). The reciprocal-space range used was $1.0 \le Q \le 25\,\text{Å}^{-1}$ for the X-ray data and $0.7 \le Q \le 45\,\text{Å}^{-1}$ for the neutron data. This excludes most of the diffuse magnetic contribution to the neutron data, which peaks at $0.4\,\text{Å}^{-1}$ [24] and was barely observed above background in our high-Q-optimised measurement. All PDF analysis was performed using the PDFGui program [40] by refinement to both X-ray and neutron PDFs over the range $0 < r < 10\,\text{Å}$, with a weighting factor chosen so that both datasets sets contributed approximately equally.

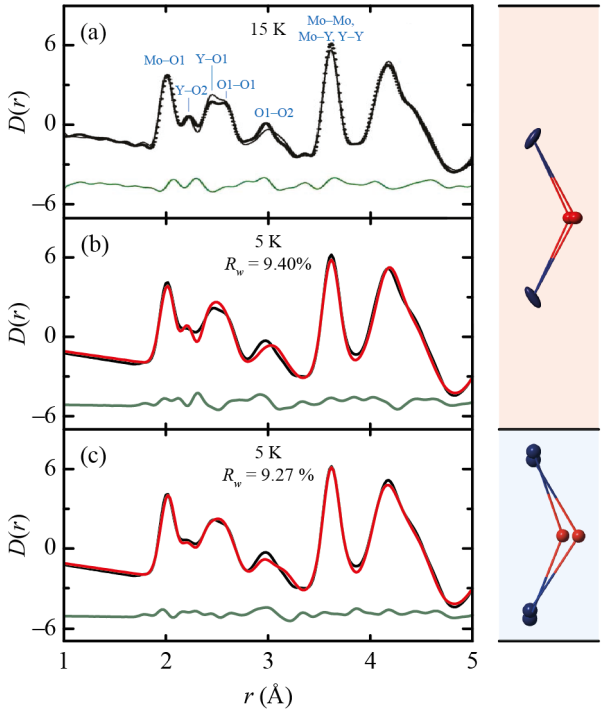

FIG. 2: (a) Reproduction of the fit to neutron PDF data shown in Fig. 8 of [29] for the split-site model described in the text. (b) Fit of the split-site model to our neutron PDF data. (c) Fit of the orbital-dimer model ($I4_1md$; described in the text) to our neutron PDF data. In (a), data are shown as points and fit as a line; in (b) and (c), data are shown as black lines, fits as red lines, and data−fit as green lines. The extrema of Mo–O1–Mo conformations accounted for by each model are shown beside the corresponding fit.

In the previous PDF study [29], the local structure of $Y_2Mo_2O_7$ was modelled using the conventional $Fd\bar{3}m$ structure with O1 sites partitioned equally between two sites (O1a,O1b) generated from the fractional coordinates $(x, 1/8, 1/8)$ with different x; we call this the "split-site model". We first checked that we could reproduce the fit obtained in [29] using this model and our new data. We found that stable refinement required the use of constraints on the anisotropic displacement parameters for the O1a/O1b sites—hence we have marginally fewer parameters than [29] (see SI). Nevertheless our fit for the split-site model is essentially indistinguishable from that in [29] [Fig. 2(a,b)]; values of refined parameters are compared in Table I. We conclude that our sample, data, and refinement procedures are consistent with

TABLE I: Structural parameters for our PDF refinements using the split-site and orbital-dimer models. Reference values from the split-site refinements of [29] are shown in italics (* = Rietveld and † = PDF refinements; note that the consistency in cell parameters is typical for Rietveld/PDF comparisons). Lattice parameters are given in Å and displacement parameters in 10^{-2} Å^2.

Split-site model [29]			**Orbital dimer model**	
a	10.2255(10)	*10.20753(2)**	$c_\mathrm{t} \equiv \sqrt{2}a_\mathrm{t}$	10.2269(10)
x(O1a)	0.3320(6)	*0.3305(12)†*	y(Mo)	0.7371(8)
x(O1b)	0.3446(6)	*0.3465(13)†*	z(O1a)	0.6938(6)
U_{11}(Y)	0.512(15)	*0.471(7)**	x(O1b)	0.7184(5)
U_{12}(Y)	−0.129(19)	*−0.136(9)**	y(O1b)	0.7910(5)
U_{11}(Mo)	1.39(5)	*1.1(1)**	z(O1b)	0.2467(4)
U_{12}(Mo)	0.93(5)	*0.83(2)**	z(O1c)	0.2709(6)
U_{11}(O1)	1.02(11)	*1.45(2)**	U_iso(Y)	0.355(11)
U_{22}(O1)	0.81(3)	*0.66(1)**	U_iso(Mo)	1.14(5)
U_iso(O2)	0.55(3)	*0.32(2)**	U_iso(O)	0.89(2)

[29].

We now propose an alternative model of static disorder in $Y_2Mo_2O_7$. Our starting point is the observation that Mo ADPs are strongly elongated along the local-$\langle 111\rangle$ axes in the average-structure model [Fig. 1(b)]. This suggests that Mo^{4+} ions are locally displaced towards or away from the centres of Mo_4 tetrahedra. Physically-reasonable mechanisms for Mo displacements, such as charge polarisation and orbital interactions [41], require that displacements are not random but coupled. There are two basic possibilities for this coupling. It may require that all Mo on a tetrahedron displace towards its centre or all displace away ("4-in/4-out" state); alternatively, it may require that two Mo displace towards the centre and two displace away ("2-in/2-out" state). The former displacement pattern is necessarily ordered and is ruled out in $Y_2Mo_2O_7$ by the absence of global symmetry lowering. In the latter case, by contrast, the coupling is frustrated and the displacement pattern need not be ordered at all. In fact, if all 2-in/2-out states were equally probable, there would be a macroscopic degeneracy of Mo-displaced configurations analogous to the degeneracy of proton configurations in cubic water ice [42]—*i.e.*, an orbital-ice state.

To build a model that can be directly compared with the split-site model in terms of its ability to explain the experimental PDF, we consider an ordered approximant to the ensemble of disordered 2-in/2-out states. This is possible because ordered and disordered 2-in/2-out states show essentially the same PDF for distances within a single unit cell. The highest-symmetry subgroup of $Fd\bar{3}m$ that permits 2-in/2-out Mo displacements is $I4_1md$. This structure is shown in Fig. 3(a), and relates to $Fd\bar{3}m$ in the same way as the proton-ordered ice phase XIc relates to proton-disordered cubic ice Ic [43]. The tetragonal unit cell has dimensions $a_\mathrm{t} = a/\sqrt{2}$ and $c_\mathrm{t} = a$. Both Mo and Y occupy the $8b$ site at $(0, y, z)$, O2 occupies the $4a$ site at $(0, 0, z)$, and the O1 site is split into three sites: O1a and O1c also occupy the $4a$ site and O1b occupies the $16c$ site at (x, y, z). The Mo point symmetry is lowered from $\bar{3}m$ to m, which is consistent with a Jahn-Teller-type distortion of the d^2 electronic configuration of Mo^{4+}.

We reduce the number of refined parameters in our $I4_1md$ model to match the split-site model in the following way. First, we constrain the ratio of unit-cell dimensions $c_\mathrm{t} = \sqrt{2}a_\mathrm{t}$, so that the parent cell remains metrically cubic. Second, the small displacement parameters of the Y and O2 sites indicate that they are not strongly disordered [Fig. 1(c)]; we therefore fix them at their average-structure positions of $(0, \frac{3}{4}, \frac{1}{8})$ and (0,0,0), respectively. Finally, the $I4_1md$ structure allows for Mo displacements within the plane that contains the cubic local-$\langle 111\rangle$ axis (towards or away from the tetrahedron centre) and local-$\langle 110\rangle$ axis (towards or away from neighbouring Mo lying on the same mirror plane). Consequently, two parameters are needed to define the Mo displacement direction, which would increase the number of parameters beyond the split-site model. Such a refinement was stable, however, and showed that the dominant displacement direction is actually the local-$\langle 110\rangle$. Subsequently, we fixed the local-$\langle 111\rangle$ component at zero ($z(\mathrm{Mo}) \equiv \frac{5}{8}$), so that the number of parameters was identical to the split-site model. We call this constrained $I4_1md$ model the "orbital dimer" model.

We refined this model against neutron and X-ray PDF data using PDFGui [40]. The fit to neutron data is presented in Fig. 2(c); values of refined parameters are given in Table I, and the fit to X-ray data is given in SI. The quality of fit for the orbital-dimer model is higher than for the split-site model ($R_\mathrm{wp} = 9.27\%$ *vs.* 9.40%) despite employing the same number of structural parameters. Moreover, the orbital-dimer model accounts more convincingly for the low-r peaks. Further evidence for improved model quality comes from the refinement statistics: whereas the split-site model showed strong covariance ($> 80\%$) between the x(O1a), x(O1b), and U_{11}(O1) parameters, the orbital-dimer refinement yielded no anomalous covariance terms; in fact, a robust refinement with $R_\mathrm{wp} = 8.29\%$ could also be achieved with more structural parameters (see SI). We therefore conclude that the absence of visible splitting of the Mo–Mo peak is not inconsistent with Mo off-centring. On the contrary, our model includes Mo displacements and robustly yields an improved fit to experimental data [Fig. 2c].

The orbital-dimer model is represented in Fig. 3. In every Mo_4 tetrahedron, two Mo are displaced towards each other and two away from each other; in each case, the refined displacement magnitude is $0.093(6)$ Å and the displacement direction is along the line connecting the Mo pair [Fig. 3(a)]. The Mo displacements thus describe a covering of the pyrochlore lattice by Mo–Mo dimers (short Mo–Mo distances), with one dimer per tetrahedron. The O1 displacements are correlated with Mo displacements as shown in Fig. 3(b). When neighbouring Mo displace towards each other, the bridging O1 displaces away from the dimer and the Mo–O1–Mo angle decreases; conversely, when neighbouring Mo displace away from each other the Mo–O1–Mo angle in-

creases. The effect of O1 displacements is to keep all Mo–O1 distances essentially the same—a result that is perhaps unsurprising on electrostatic grounds but nevertheless explains the lack of visible Mo–O1 peak splitting. Fig. 3(c) shows the distribution of atomic positions obtained by superposing the full $Fd\bar{3}m$ average-structure symmetry on the refined local-structure model. The distribution of local-$\langle 110\rangle$ Mo displacements has a larger component parallel to the local-$\langle 111\rangle$ axis than perpendicular to it, consistent with the prolate Mo displacement ellipsoid in the average-structure model [Fig. 1(b) and inset to Fig. 3(c)] (see SI). Finally, we stress that the ordered $I4_1md$ dimer covering [left panel of Fig. 3(d)] is an *approximant* to disordered dimer coverings that show the same local displacement patterns. There is a macroscopic degeneracy of disordered dimer coverings that reproduce the observed $Fd\bar{3}m$ symmetry on spatial averaging; the right panel of Fig. 3(d) shows a disordered example that more closely approximates the true structure. This is the same degeneracy responsible for the unusual physics of cubic water ice [42], spin ices [44, 45], and charge ices [46, 47].

Crucially, the orbital-dimer model is consistent with previous experimental studies and theoretical requirements for spin-glass formation. The O1 displacement gives rise to 30 distinct Y environments, consistent with the broad resonance observed in ^{89}Y NMR studies [31, 33]. The Mo displacements split the average Mo–Mo distance into long, short, and intermediate distances in the ratio 1:1:4. This static disorder makes a contribution to the variance in Mo–Mo distances of 0.012(2) Å^2, in qualitative agreement with the EXAFS result (0.026(5) Å^2); moreover, the displacement direction (parallel to Mo–Mo pairs) is consistent with EXAFS [32]. This agreement is encouraging because EXAFS should be more sensitive to Mo displacements than the PDF, in which Mo–Mo, Y–Y and Mo–Y peaks overlap and our intermediate Mo–Mo distance is similar to the average Mo–Mo distance. It has been shown that small ($\sim$10%) variations in exchange interactions may induce spin-glass transitions in geometrically-frustrated magnets [12, 13]. In $Y_2Mo_2O_7$, variations in bond angle of 9° are calculated to yield factor-of-two variations in the magnetic coupling strength [29]. Our results show that the Mo–O1–Mo angle actually varies by a significantly larger amount, 23° [Fig. 3(b)]. Importantly, the arrangement of Mo–O1–Mo bond angles is disordered; this is because the dimer covering (*i.e.*, the arrangement of short and long Mo–Mo distances) is disordered [Fig. 3(d)], and short and long Mo–Mo distances are associated with Mo–O1–Mo bond angles of 116 and 139 degrees, respectively [Fig. 3(b)]. Hence, Mo dimerisation presents a clear mechanism to generate exchange disorder responsible for spin-glass freezing. Experimentally, the width $\delta \sim 1$ T of the internal-field distribution measured by ^{89}Y NMR at 25 K [33] implies a distribution of exchange energies of approximate width $gS\mu_B\delta/k_B \approx 13$ K, which is similar to T_f, as expected theoretically [12, 13]. Theoretical studies suggest that Mo dimerisation may be explained by an orbital (Jahn-Teller) mechanism. A recent study parameterised a three-orbital Hubbard model using DFT [41], and concluded

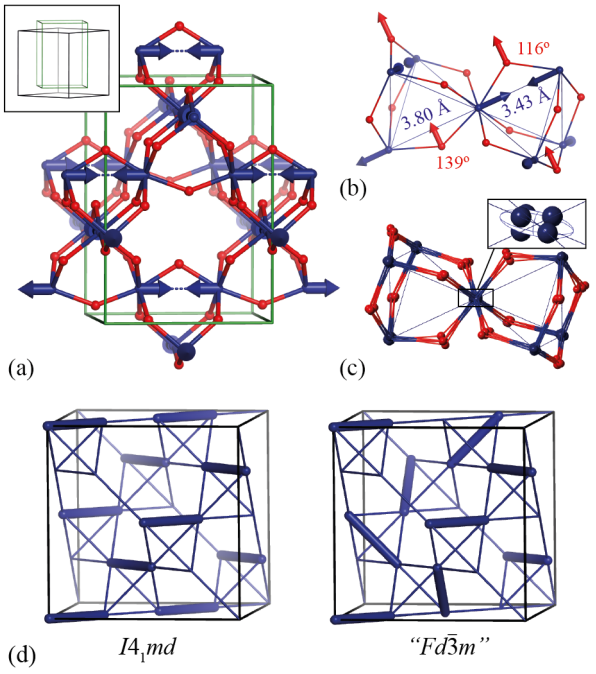

FIG. 3: (a) Representation of the orbital-dimer model obtained from PDF refinements: Mo displacements are shown as blue arrows, Mo–Mo dimers as blue dashed lines, and O1 atoms in red. The inset shows the relationship between $I4_1md$ and $Fd\bar{3}m$ unit cells. (b) Local Mo environment in the orbital-dimer model, showing Mo displacement directions (blue arrows) and dominant O1 displacement directions (red arrows). (c) Distribution of atomic positions obtained by imposing the full symmetry of the average structure. In the inset, the superposition of displaced Mo sites is compared to the prolate displacement ellipsoid obtained from Rietveld refinement. (d) Comparison of ordered and disordered coverings of the pyrochlore lattice by Mo–Mo dimers (thick blue lines). The left panel shows the ordered dimer covering for the $I4_1md$ structure, which breaks cubic symmetry. The right panel shows an example of a disordered dimer covering that more closely approximates the true orbital-ice state; spatial averaging over such dimer coverings preserves cubic symmetry.

that spin and orbital degrees of freedom are strongly coupled for the d^2 configuration and many energetically-similar spin-orbital excited states exist if the ground state is 2-in/2-out. A second DFT study relaxed the orbital and lattice configuration for different spin structures and obtained different lattice distortions in each case [48]. These studies provide compelling evidence for a strong coupling of spin, orbital, and lattice degrees of freedom. We therefore interpret the 2-in/2-out pattern of Mo displacements as the formation of orbital dimers, driven by the Jahn-Teller activity of the d^2 electronic configuration.

Our results show that the spin-glass state in $Y_2Mo_2O_7$ is driven by orbital dimerisation of Jahn-Teller active Mo^{4+} ions—a rare example where spin-glass formation is not driven by random compositional or site disorder [49]. While spin-glass formation due to non-random interactions has been studied theoretically [50], to the best of our knowledge this rep-

resents the first such example for a real spin glass. Yet, dimer states play a key role in determining other properties of materials. In LiV_2O_4, charge dimerisation on V_4 tetrahedra may explain the observed heavy-fermion behaviour [51]. In Ba_2YMoO_6, Mo^{5+} spins freeze into a disordered arrangement of spin-singlet dimers [52], while in $CuIr_2O_4$ Ir^{3+}/Ir^{4+} charge ordering accompanies spin dimerisation [53]. Dimer models may be relevant to other molybdate pyrochlores; *e.g.*, $Lu_2Mo_2O_7$ [54], $Tb_2Mo_2O_7$ [55, 56], and $Dy_2Mo_2O_7$ [57]. Interestingly, our model of Mo displacements resembles models of Nb displacements in (non-magnetic) niobate pyrochlores [58, 59], suggesting that the proximity of both materials to a metal-insulator transition may be related to orbital dimerisation [60, 61]. Our results suggest three promising directions for future work on $Y_2Mo_2O_7$. First, a comprehensive single-crystal diffuse scattering study would indicate the extent to which a particular subset of dimer coverings is preferentially selected. Second, analysis of the distribution of magnetic couplings may allow a consistent interpretation of puzzling magnetic diffuse-scattering data [48]. Third, the orbital-dimer state we propose should collapse at sufficiently high temperature; *i.e.*, an orbital-ice to orbital-liquid [62, 63] transition may be anticipated.

We thank A. Simonov, J. R. Stewart, M. Mourigal, C. R. Wiebe, H. J. Silverstein, M. J .P. Gingras, F. Flicker, and J. S. Gardner for useful discussions. We acknowledge the Rutherford Appleton Laboratory for access to the ISIS Neutron Source. This research used resources of the Advanced Photon Source, a U.S. Department of Energy (DOE) Office of Science User Facility operated for the DOE Office of Science by Argonne National Laboratory under Contract No. DE-AC02-06CH11357. P.M.M.T., J.A.M.P., and A.L.G. acknowledge financial support from the STFC, E.P.S.R.C. (EP/G004528/2), and the E.R.C. (Grant Ref: 279705).

* Electronic address: paddison@gatech.edu

[1] S. J. Blundell, *Magnetism in Condensed Matter* (Oxford University Press, Oxford, 2001).
[2] J. A. Mydosh, *Rep. Prog. Phys.* **78**, 052501 (2015).
[3] D. Sherrington, S. Kirkpatrick, *Phys. Rev. Lett.* **35**, 1792 (1975).
[4] B. Barbara. A. P. Malozemoff, Y. Imry, *Phys. Rev. Lett.* **47**, 1852 (1981).
[5] K. Binder, A. P. Young, *Rev. Mod. Phys.* **58**, 801 (1986).
[6] C. Y. Huang, *J. Magn. Magn. Mater.* **51**, 1 (1985).
[7] L. Lundgren, P. Svedlindh, P. Nordblad, O. Beckman, *Phys. Rev. Lett.* **51**, 911 (1983).
[8] U. Atzmony, E. Gurewitz, M. Melamud, H. Pinto, H. Shaked, G. Gorodetsky, E. Hermon, R. M. Hornreich, S. Shtrikman, B. Wanklyn, *Phys. Rev. Lett.* **43**, 782 (1979).
[9] P. Schiffer, A. P. Ramirez, D. A. Huse, P. L. Gammel, U. Yaron, D. J. Bishop, A. J. Valentino, *Phys. Rev. Lett.* **74**, 2379 (1995).
[10] C. R. Wiebe, J. E. Greedan, P. P. Kyriakou, G. M. Luke, J. S. Gardner, A. Fukaya, I. M. Gat-Malureanu, P. L. Russo, A. T. Savici, Y. J. Uemura, *Phys. Rev. B* **68**, 134410 (2003).
[11] E. M. Benbow, N. S. Dalal, S. E. Latturner, *J. Am. Chem. Soc.* **131**, 3349 (2009).
[12] T. E. Saunders, J. T. Chalker, *Phys. Rev. Lett.* **98**, 157201 (2007).
[13] A. Andreanov, J. T. Chalker, T. E. Saunders, D. Sherrington, *Phys. Rev. B.* **81**, 014406 (2010).
[14] A. D. LaForge, S. H. Pulido, R. J. Cava, B. C. Chan, A. P. Ramirez, *Phys. Rev. Lett.* **110**, 017203 (2013).
[15] J. S. Gardner, M. J. P. Gingras, J. E. Greedan, *Rev. Mod. Phys.* **82**, 53 (2010).
[16] M. J. P. Gingras, C. V. Stager, N. P. Raju, B. D. Gaulin, J. E. Greedan, *Phys. Rev. Lett.* **78**, 947 (1997).
[17] M. J. P. Gingras, C. V. Stager, B. D. Gaulin, N. P. Raju, J. E. Greedan, *J. Appl. Phys.* **79**, 6170 (1996).
[18] K. Blacklock, H. W. White, E. Gürmen, *J. Chem. Phys.* **73**, 1966 (1980).
[19] N. P. Raju, E. Gmelin, R. K. Kremer, *Phys. Rev. B* **46**, 5405 (1992).
[20] K. Miyoshi, Y. Nishimura, K. Honda, K. Fujiwara, J. Takeuchi, *J. Phys. Soc. Jpn.* **69**, 3517 (2000).
[21] N. Ali, P. Hill, X. Zhang, F. Willis, *J. Alloys Comp.* **181**, 281 (1992).
[22] V. Dupuis, E. Vincent, J. Hammann, J. E. Greedan, A. S. Wills, *J. Appl. Phys.* **91**, 8384 (2002).
[23] F. Ladieu, F. Bert, V. Dupuis, E. Vincent, J. Hammann, *J. Phys.: Condens. Matter* **16**, S735 (2004).
[24] J. S. Gardner, B. D. Gaulin, S.-H. Lee, C. Broholm, N. P. Raju, J. E. Greedan, *Phys. Rev. Lett.* **83**, 211 (1999).
[25] S. R. Dunsiger, R. F. Kiefl, K. H. Chow, B. D. Gaulin, M. J. P. Gingras, J. E. Greedan, A. Keren, K. Kojima, G. M. Luke, W. A. MacFarlane, N. P. Raju, J. E. Sonier, Y. J. Uemura, W. D. Wu, *J. Appl. Phys.* **79**, 6636 (1996).
[26] J. Gardner, G. Ehlers, R. Heffner, F. Mezei, *J. Magn. Magn. Mater.* **226–230, Part 1**, 460 (2001).
[27] J. S. Gardner, G. Ehlers, S. T. Bramwell, B. D. Gaulin, *J. Phys.: Condens. Matter* **16**, S643 (2004).
[28] J. N. Reimers, J. E. Greedan, M. Sato, *J. Solid State Chem.* **72**, 390 (1988).
[29] J. E. Greedan, D. Gout, A. D. Lozano-Gorrin, S. Derahkshan, T. Proffen, H.-J. Kim, E. Božin, S. J. L. Billinge, *Phys. Rev. B* **79**, 014427 (2009).
[30] L. Minervini, R. W. Grimes, Y. Tabira, R. L. Withers, K. E. Sickafus, *Philos. Mag. A* **82**, 123 (2002).
[31] A. Keren, J. S. Gardner, *Phys. Rev. Lett.* **87**, 177201 (2001).
[32] C. H. Booth, J. S. Gardner, G. H. Kwei, R. H. Heffner, F. Bridges, M. A. Subramanian, *Phys. Rev. B* **62**, R755 (2000).
[33] O. Ofer, A. Keren, J. S. Gardner, Y. Ren, W. A. MacFarlane, *Phys. Rev. B* **82**, 092403 (2010).
[34] E. Sagi, O. Ofer, A. Keren, J. S. Gardner, *Phys. Rev. Lett.* **94**, 237202 (2005).
[35] M. Sato, X. Yan, J. E. Greedan, *Z. Anorg. Allg. Chem.* **540**, 177 (1986).
[36] J. E. Greedan, M. Sato, X. Yan, F. S. Razavi, *Solid State Commun.* **59**, 895 (1986).
[37] S. Hull, R. I. Smith, W. I. F. David, A. C. Hannon, J. Mayers, R. Cywinski, *Physica B* **180–181, Part 2**, 1000 (1992).
[38] A. K. Soper, E. R. Barney, *J. Appl. Crystallogr.* **44**, 714 (2011).
[39] A. C. Hannon, W .S. Howells, A. K. Soper, *IOP Conference Series* **107** 193 (1990). (Proceedings of the Conference on Neutron Scattering Data Analysis 1990, ed. M. W. Johnson.)
[40] C. L. Farrow, P. Juhas, J. W. Liu, D. Bryndin, E. S. Božin, J. Bloch, T. Proffen, S. J. L. Billinge, *J. Phys.: Condens. Matter* **19**, 335219 (2007).
[41] H. Shinaoka, Y. Motome, T. Miyake, S. Ishibashi, *Phys. Rev. B* **88**, 174422 (2013).
[42] L. Pauling, *J. Am. Chem. Soc.* **57**, 2680 (1935).

[43] Z. Raza, D. Alfe, C. G. Salzmann, J. Klimes, A. Michaelides, B. Slater, *Phys. Chem. Chem. Phys.* **13**, 19788 (2011).

[44] S. T. Bramwell, M. J. P. Gingras, *Science* **294**, 1495 (2001).

[45] H. D. Zhou, C. R. Wiebe, J. A. Janik, L. Balicas, Y. J. Yo, Y. Qiu, J. R. D. Copley, J. S. Gardner, *Phys. Rev. Lett.* **101**, 227204 (2008).

[46] D. P. Shoemaker, R. Seshadri, A. L. Hector, A. Llobet, T. Proffen, C. J. Fennie, *Phys. Rev. B* **81**, 144113 (2010).

[47] V. E. Fairbank, A. L. Thompson, R. I. Cooper, A. L. Goodwin, *Phys. Rev. B* **86**, 104113 (2012).

[48] H. J. Silverstein, K. Fritsch, F. Flicker, A. M. Hallas, J. S. Gardner, Y. Qiu, G. Ehlers, A. T. Savici, Z. Yamani, K. A. Ross, B. D. Gaulin, M. J. P. Gingras, J. A. M. Paddison, K. Foyevtsova, R. Valenti, F. Hawthorne, C. R. Wiebe, H. D. Zhou, *Phys. Rev. B* **89**, 054433 (2014).

[49] E. A. Goremychkin, R. Osborn, B. D. Rainford, R. T. Macaluso, D. T. Adroja, M. Koza, *Nat. Phys.* **4**, 766 (2008).

[50] J. Villain, *J. Phys. C* **10**, 1717 (1977).

[51] P. Fulde, A. N. Yaresko, A. A. Zvyagin, Y. Grin, *EPL* **54**, 779 (2001).

[52] M. A. de Vries, A. C. Mclaughlin, J.-W. G. Bos, *Phys. Rev. Lett.* **104**, 177202 (2010).

[53] P. G. Radaelli, Y. Horibe, M. J. Gutmann, H. Ishibashi, C. H. Chen, R. M. Ibberson, Y. Koyama, Y.-S. Hor, V. Kiryukhin, S.-W. Cheong, *Nature* **416**, 155 (2002).

[54] L. Clark, G. J. Nilsen, E. Kermarrec, G. Ehlers, K. S. Knight, A. Harrison, J. P. Attfield, B. D. Gaulin, *Phys. Rev. Lett.* **113**, 117201 (2014).

[55] B. D. Gaulin, J. N. Reimers, T. E. Mason, J. E. Greedan, Z. Tun, *Phys. Rev. Lett.* **69**, 3244 (1992).

[56] D. K. Singh, J. S. Helton, S. Chu, T. H. Han, C. J. Bonnoit, S. Chang, H. J. Kang, J. W. Lynn, Y. S. Lee, *Phys. Rev. B* **78**, 220405 (2008).

[57] T. Katsufuji, H. Y. Hwang, and S-W. Cheong, *Phys. Rev. Lett.* **84**, 1998 (2000).

[58] T. M. McQueen, D. V. West, B. Muegge, Q. Huang, K. Noble, H. W. Zandbergen, R. J. Cava, *J. Phys.: Condens. Matter* **20**, 235210 (2008).

[59] S. Torigoe, Y. Ishimoto, Y. Aoishi, H. Murakawa, D. Matsumura, K. Yoshii, Y. Yoneda, Y. Nishihata, K. Kodama, K. Tomiyasu, K. Ikeda, H. Nakao, Y. Nogami, N. Ikeda, T. Otomo, N. Hanasaki, *Phys. Rev. B.* **93**, 085109 (2016).

[60] P. Blaha, D. J. Singh, K. Schwarz, *Phys. Rev. Lett.* **93**, 216403 (2004).

[61] N. Hanasaki, K. Watanabe, T. Ohtsuka, I. Kézsmárki, S. Iguchi, S. Miyasaka, Y. Tokura, *Phys. Rev. Lett.* **99**, 086401 (2007).

[62] G. Khaliullin and S. Maekawa, *Phys. Rev. Lett.* **85**, 3950 (2000).

[63] S. Nakatsuji, K. Kuga, K. Kimura, R. Satake, N. Katayama, E. Nishibori, H. Sawa, R. Ishii, M. Hagiwara, F. Bridges, T. U. Ito, W. Higemoto, Y. Karaki, M. Halim, A. A. Nugroho, J. A. Rodriguez-Rivera, M. A. Green, C. Broholm, *Science* **336**, 559 (2012).